MATHEMATICAL, PHYSICAL, AND ENGINEERING SCIENCES

IMAGING OF PHASE OBJECTS WITH A SEMICONDUCTOR LASER CONFOCAL MICROSCOPE

CAESAR A. SALOMA
National Institute of Physics, College of Science
University of the Philippines Diliman
1101 Quezon City

ABSTRACT

A reflecting-type semiconductor laser confocal microscope is developed and used to image thin phase objects at microscopic transverse resolutions. Phase objects have negligible absorption characteristics and therefore can not be observed using bright-field imaging. Biological samples are essentially phase objects when microscopically observed in situ or in vivo. In this paper, phase objects of varying optical thickness are developed from high-quality microscope cover glasses.

To discriminate phase objects of different optical thickness $l = n_s d$, where n_s is the refractive index of the sample and d is its geometrical thickness, the confocal microscope utilizes both the sensitivity of the laser output to optical feedback and the optical sectioning capability of confocal imaging optics. The output power of the laser is monitored directly using the built-in photodiode in the commercially-available laser package. This detection scheme makes the laser confocal microscope compact, easy to align, and inexpensive to build.

To determine the optical thickness of a sample, we measure the amount of defocusing that results when it is introduced into the path of a beam that is focused initially on a plane mirror. In the absence of a sample, optical feedback is maximum and the photodiode output is maximum. Defocusing decreases the amount of feedback light that is returned by the mirror to the laser cavity.

INTRODUCTION

In this work, we demonstrate the imaging and the refractive index distribution of nonabsorbing biological samples using a semiconductor laser confocal microscope. The task involves the measurement of the optical thickness at microscopic transverse resolution. Unlike in previous approaches[1-3], interferometric principles are not utilized so length measurements can be made with less optical components. When its geometrical thickness is known a priori, the technique can be used to determine the refractive index of the sample, and vice-versa.

The optical sectioning capability of a laser confocal microscope[4] is utilized to measure the optical thickness of a sample that is placed in the path of a probe beam that is initially focused unto a plane mirror. The index mismatch at the interface of the sample and the surrounding medium defocuses the beam away from the mirror and decreases the amount of detectable light in the confocal microscope. A commercially-available semiconductor laser (SL) is utilized as a light source. The SL output is modulated by the amount of optical feedback that is returned by the mirror to the laser cavity. It has long been known that the SL output power and wavelength are both sensitive to optical feedback[5].

In transmission-type optical microscopy, SL's have proven to be a versatile light source particularly in reducing image speckles through coherence modulation[6-7]. Feedback sensitivity has also been utilized recently[8-9] to construct a reflecting-type SL confocal microscope that is compact, easy to align, and economical to build. Under weak feedback[10], the magnitude of the feedback field and therefore the sample amplitude reflectivity, becomes directly proportional to the SL output power[11-12] in the built-in photodiode (PD) in the laser package.

A similar SL confocal microscope design is adapted in our technique. Due to defocusing, the presence of a transparent sample reduces the amount of feedback to the SL cavity and decreasing the generated PD current. The optical thickness is deduced from the axial displacement that the mirror must be given to recover maximum PD current. Because a confocal microscope has a narrow axial point spread function, optical feedback decreases rapidly with defocusing, our technique is sensitive even to small thickness differences.

THEORY

Illustrated in Fig. 1 is the optical configuration employed to measure the optical thickness $l_s = n_s d$, of a transparent sample of refractive index n_s and geometrical thickness d. Without the sample, the SL output beam focuses towards the plane mirror and optical feedback to the laser cavity is maximum. The refraction at the air-sample interface defocuses the beam away from the mirror and reduces the amount of optical feedback. The separation distance z between the mirror and the (virtual) focus depends on $n_s d$, and the numerical aperture NA of the objective lens. The SL output power is directly proportional to the generated PD current.

Optical feedback affects the amplitude reflectivities r and r', of the laser cavity mirrors[11]. According to the compound mirror analysis of Wilson, et al.[8-9], feedback increases the value of reflectivity r by an amount $\delta r = (1 - r^2)\gamma$, where γ is the ratio between the magnitudes of the feedback field and the original (feedback-free) SL output field. Under weak feedback, any variation in the value of r leads to a proportional change in the SL output power.

If the feedback contribution from other optical interfaces in the setup, is independent of the axial position z of the mirror then any variation δr can arise only

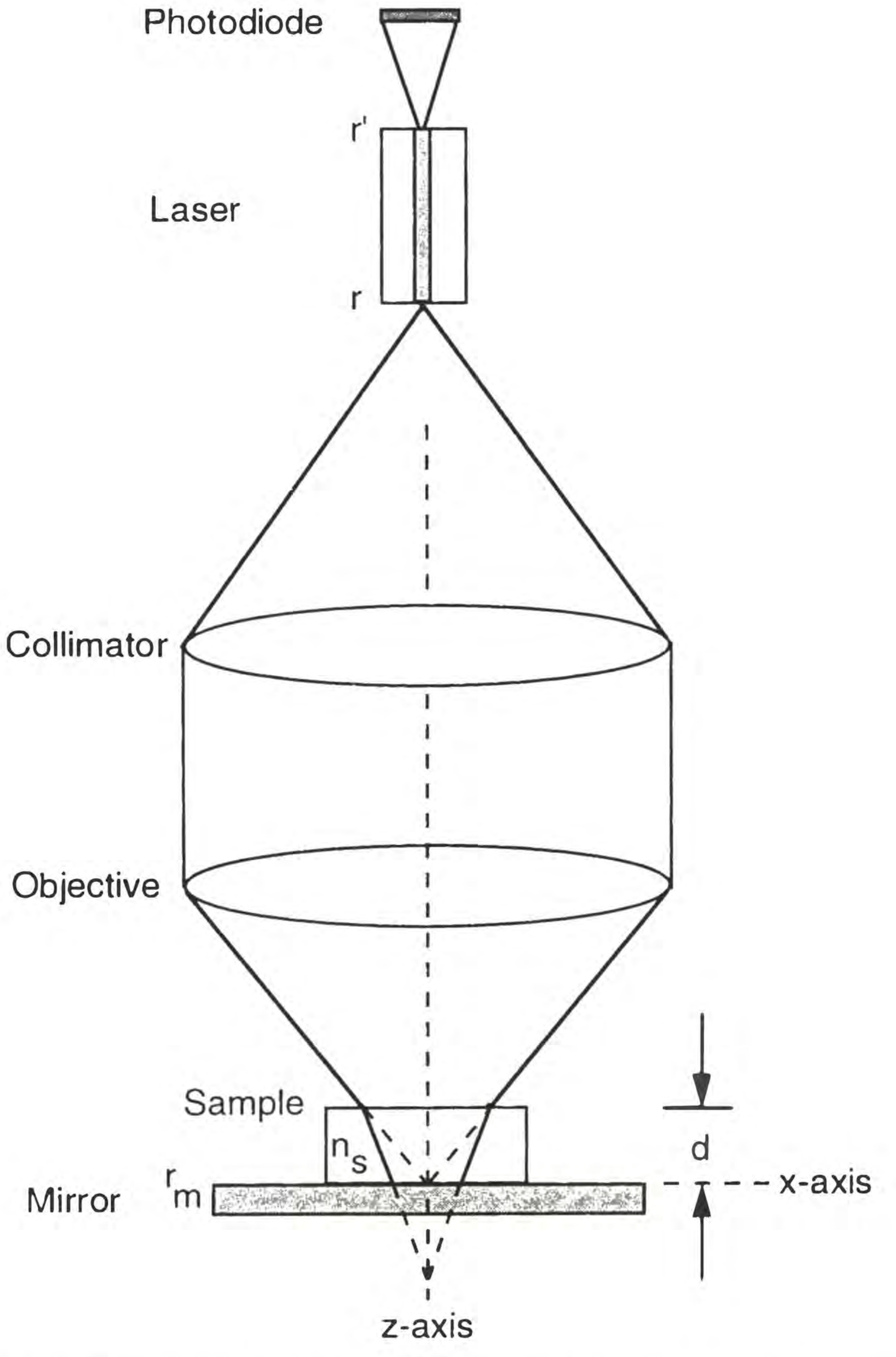

Figure 1. Optical set-up for measuring the optical thickness $l_s = n_s d$, of a transparent sample of geometrical thickness d, and refractive index n_s. The SL power output can be monitored directly from the PD current, where r_m, r, and r' are the reflectivities of the mirror and the SL cavity facets, respectively.

from changes in the light reflected by the mirror itself. The value of γ (and or r) varies only with the separation distance z between the beam focus and the mirror.

Axially-scanning the mirror away from the beam focus decreases the PD current $I_{PD}(z)$ from its peak (in-focus) value, in a manner that describes the effective axial intensity point spread function $h^2(z)$ of the confocal microscope, where $h(z)$ is the amplitude axial point spread function[8-9]. This implies that to within a multiplicative constant: $I_{PD}(z) = h^2(z)$ where the mirror reflectivity is $r_m = 1$.

Similarly, the introduction a sample into the focused beam, also causes the $I_{PD}(z = 0)$ to decrease from its peak value. Maximum feedback is recovered, if the mirror is displaced axially by a distance z_F from its original position at $z = 0$, where:

$$z_F = d\,\frac{\left(\tan\alpha\cot\ \sin^{-1}\frac{n_a\sin\alpha)}{n_s} - 1\right)}{\left(\tan\alpha\cot\ \sin^{-1}\frac{n_a\sin\alpha)}{n_s}\right)} \tag{1}$$

and $n_a\sin\alpha = n_s\sin\beta$, n_a being the refractive index of the surrounding medium (see Fig. 2). For samples of the same n_s, the value of z_F increases proportionately with d. However, for samples of the same thickness, the displacement z_F exhibits a nonlinear dependence with n_s. The index n_s can be measured (along the x-axis) at a spatial (transverse) resolution $\delta x = 2d\tan\beta$.

The depth of field z_P of the focused beam defines the smallest thickness δd that can be possibly measured. When the collimated beam illuminates uniformly the entire objective lens aperture then $\delta d = n_s\lambda/NA^2$. In practice however, the correct δd value is deduced directly from the effective axial response $I_{PD}(z)$ because an SL does not produce a collimated beam output profile that is circularly-symmetric that can uniformly illuminate the objective aperture. Note that the actual value of $\sin\alpha$ can be deduced from δd using the Rayleigh resolution criterion (for example).

EXPERIMENTS

A. Characteristics of the Imaging System

Measurements were performed using two semiconductor lasers (V-channeled substrate inner stripe) that emit at different (nominal) output wavelengths[12]: λ (30 mW output) = 830 nm for Sharp LTO15MF, and λ (30 mW output) = 780 nm for Sharp LTO25MF. The SL's are also known to exhibit different output beam profiles[12]. The threshold current (at 25 deg-C) for LTO15MF and LTO25MF, are 60 mA and 70 mA, respectively. Both SL's have a maximum output of 40 mW.

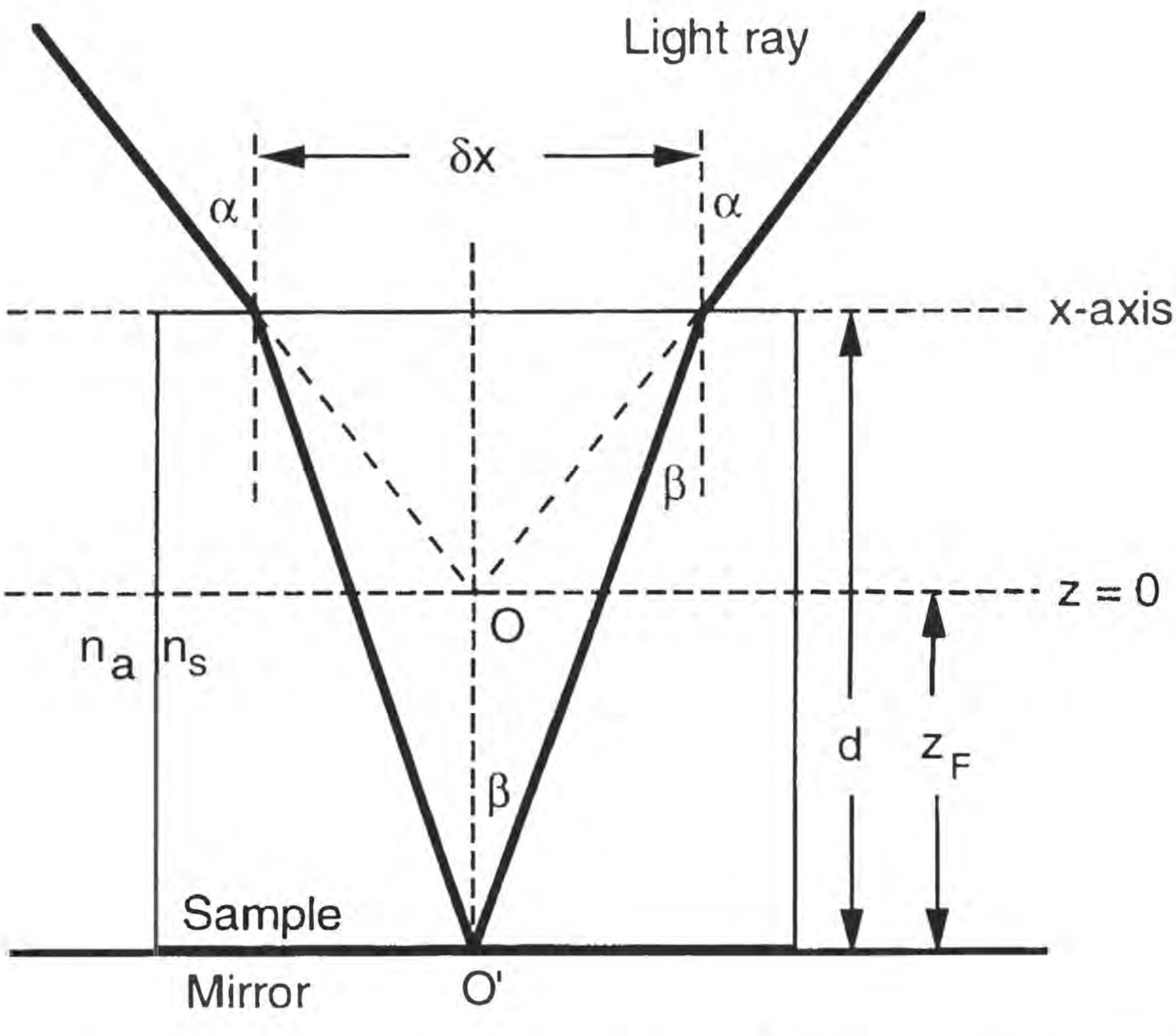

Figure 2. Geometry illustrating the relation between displacement z_F, geometrical thickness d, indexes n_s and n_a, transverse resolution δx, and the incident angle α where $n_a \sin\alpha = n_s \sin\beta$.

No active thermal control was employed during experiments, although each SL package had an extended metal base that served as a natural heatsink. The SL's were driven under constant injection current I_b by a diode laser driver (Melles-Griot Mo. 06DLD 201; resolution = 0.1 mA, noise < 1 μA, 10 MHz bandwidth). The generated PD current I_{PD} was measured at a resolution of 1 μA using the same SL driver.

A pair of 10 X achromatic objectives (NA = 0.25, working distance = 6 mm, cover glass correction = 0 mm; Sigma Koki Corp.) was used in the confocal set-up. The size of the SL package prevented the use of collimating objectives with shorter working distances, and the working distance of the objective determines the maximum d value that can be accommodated in the sample space. An aluminum-coated plane mirror with 63.28 nm-flatness, was utilized to provide optical feedback and to hold the transparent sample. The sample can be scanned along the transverse x and y directions, at a micrometer resolution of 10 μm. Scanning along the z-axis can be done at a maximum resolution of 0.5 μm.

Figures 3a-b describe the relation the maximum PD current I_{PD} (z = 0) and the injection current I_b for LTO15MF and LTO25MF, respectively. the measurements were taken in the absence of a sample, and with the mirror coinciding with the beam focus at z = 0. For both SL's, a linear dependence (curve A) exists between I_{PD} (z = 0) and current I_b. Curves B which were obtained with the mirror covered, illustrates the effect of unwanted (background) feedback on the measured PD signal. The PD currents were stable to less than 1 μA. A setting time of about 1 minute after SL start-up, was allowed before all the measurements were taken.

Curves C plot the difference between curves A and B. For both SL's, the effect of unwanted feedback on the SL output exhibits a threshold before increasing monotonously with I_b. The efficiency of monitoring the feedback change caused by sample introduction, decreases at larger injection currents, so that z_F is best determined at lower I_b values where background is weak. Operating at low optical feedback also prevents the SL spectrum from possibly exhibiting chaotic multimode characteristics[13-14].

Figures 4a-b illustrate the behavior of $I_{PD}(z)$ for different I_b values for both LTO15MF and LTO25MF The background-corrected curves represent the axial point spread function $h^2(z)$ of the confocal microscope. The data points in the $I_{PD}(z)$ curves, were sampled at intervals of 10 μm from z = 0. The curve peaks at z = 0, were located at an accuracy of 0.5 μm. For comparison, we also show the axial response $I_{Th}(z)$ of a uniformly illuminated objective aperture (NA = 0.25) for λ = 830 nm (Fig. 5a), and λ = 750 nm (Fig. 5b.). The ideal response is[4, 8]. $I_{Th}(z) = \kappa l\sin(u/2)/$ $u/2)l$ where $u = (8\pi/\lambda)z\sin^2(\alpha/2)$, and κ is a multiplicative constant.

The $I_{PD}(z)$ curves are broader than their respective $I_{Th}(z)$ curves, because the collimated SL beams could not uniformly illuminate the objective aperture. Moreover, the $I_{PD}(z)$ curves in Fig. 4a are narrower than those in Fig. 4b because LTO15MF produces a bigger beam cross-section[12] than LTO2MF. For each laser, the beam profile also varies with the I_b value[12]. Deviations from the ideal behavior

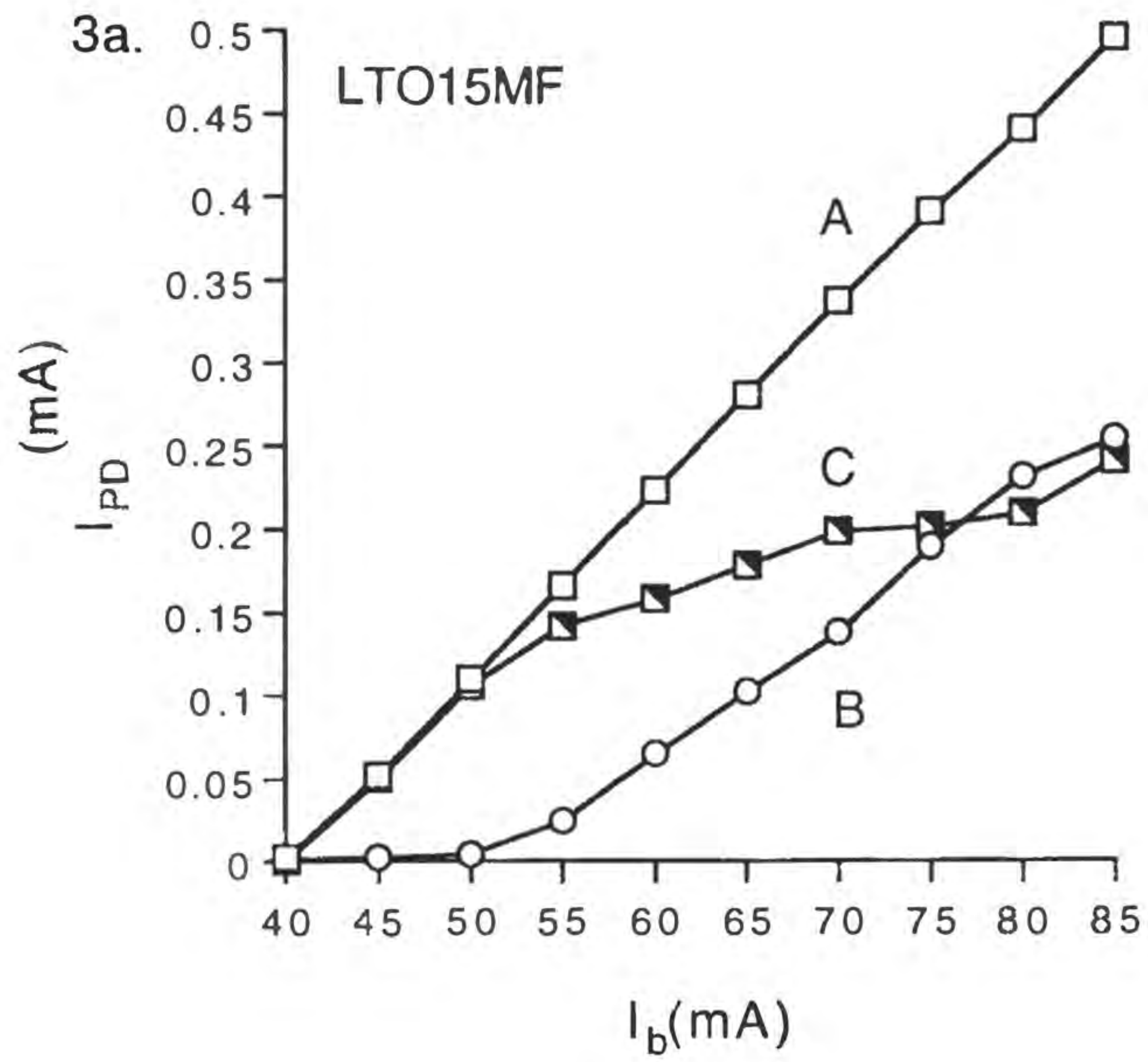

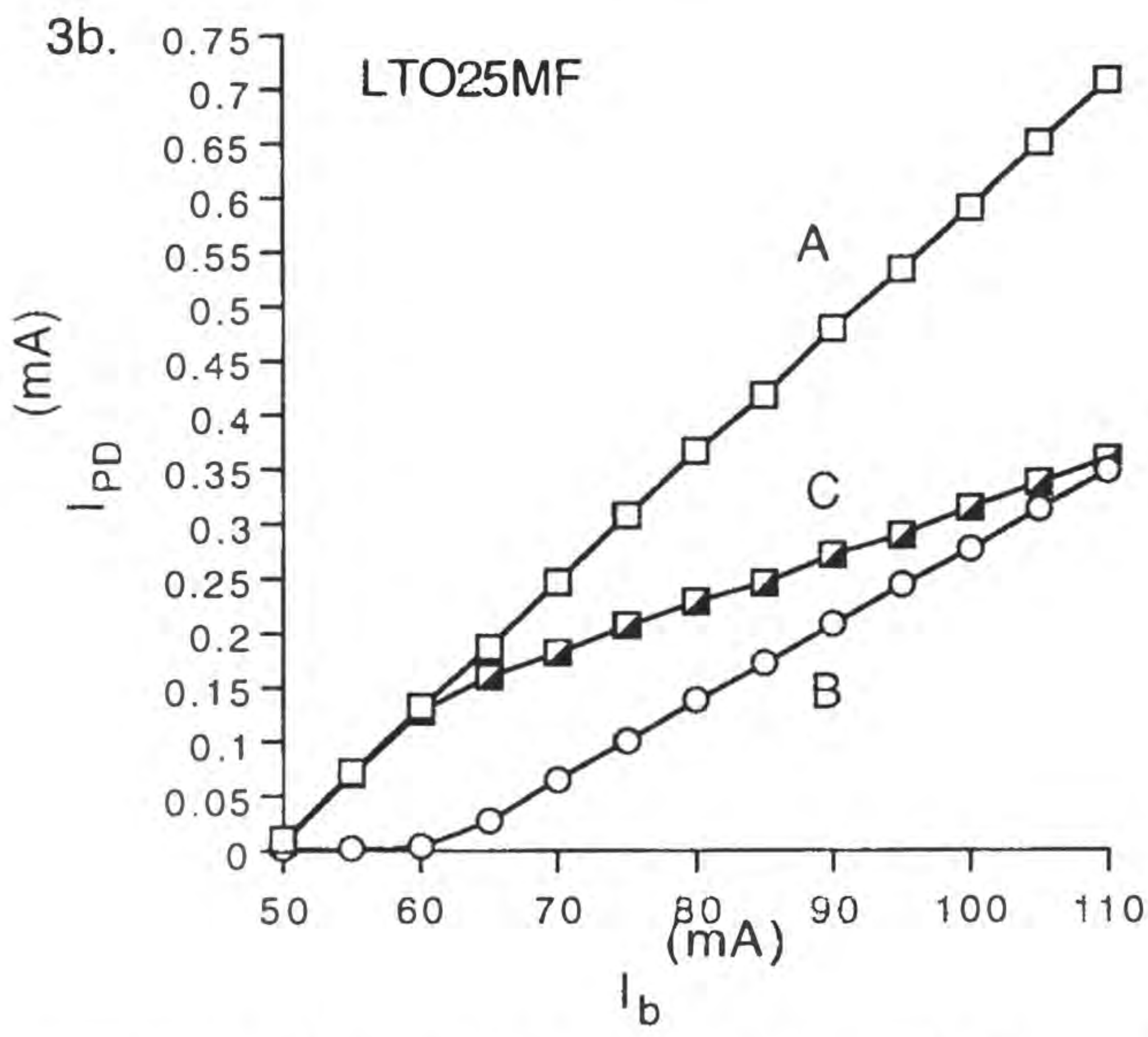

Figure 3. Dependence of $I_{PD}(z = 0)$ with injection current I_b: a)LTO15MF, and b) LTO25MF. Measurements correspond to maximum and with no sample present (NA = 0.25). Curve A depicts the behavior of $I_{PD}(z = 0)$ when the feedback contributions from the various optical interfaces in the microscope are all taken into account. Curve B depicts only the contribution of unwanted (background) feedback on $I_{PD}(z = 0)$. Curve C is the difference between curves A and B.

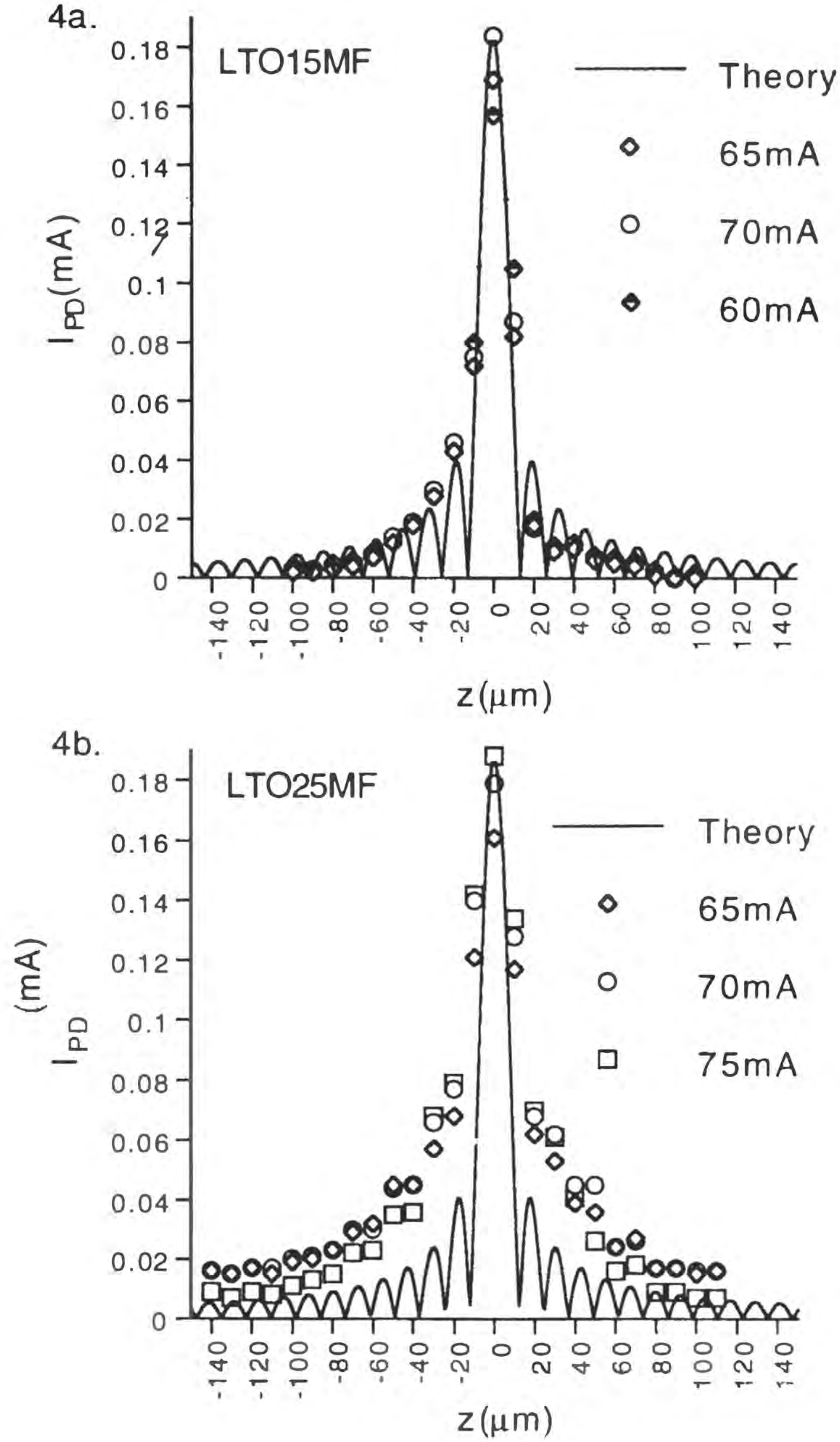

Figure 4. Background-corrected axial response $I_{PD}(z)$ as a function of injection current I_b: (a) LTO15MF, and (b) LTO25MF. The solid curves represent the axial responses of a uniformly illuminated objective (NA = 0.25).

are caused by the circular-asymmetry of the SL beam output profile[9] and to a lesser extent, by spherical aberration.

We have also verified that the unwanted feedback contribution from optical interfaces other than the mirror itself, is independent of z and varies only with I_b.

B. Optical Thickness Measurements

We investigated the accuracy of Eq. (1) by measuring the displacements z_F that corresponds to a set of 8 microscope cover glasses (Matsunami Glass Industry, Ltd.) of different geometrical thicknesses (see Table 1)[15]. The (averaged) thicknesses $\langle d \rangle$ of the sample areas probed in the experiments were also measured with a micrometer screw (resolution = 10 µm, cross-section diameter = 5 mm). Some of the $\langle d \rangle$values we interpolated between the nearest micrometer scales. Product specifications[15] also indicate a surface flatness of 7 µm, and a refractive index of $n_s = 1.523$ (alkaline content: 0.07 mg Na_2O) for the glasses.

In Fig. 5a. are raw-data curves (obtained using LTO15MF) describing the behavior of $I_{PD}(z)$ in the presence of sample no. 00 for different I_b values. The peaks of the $I_{PD}(z)$ curves were all shifted by 26 µm from $z = 0$, implying that effects arising from possible variation of λ with I_b, are not perceptible. The reflection at the air-glass interface results only in small reductions (< 10 µA) of the $I_{PD}(z)$ peak values relative to their respective sample-free $I_{PD}(z)$ profiles (see Fig. 5). The results show that the axial response profile of the confocal microscope is preserved in the presence of the glass sample no. 00.

In Fig. 5b. are background-corrected $I_{PD}(z)$ curves corresponding to presence of cover glasses nos. 00, 1, 1S, and 5, respectively ($I_b = 75$ mA). Even though the thickness of sample no. 1 and 1S differs only by about 8 µm (refer to Table), the peaks of the coresopnding $I_{PD}(z)$ curves, are still clearly discernible from each other.

Shown in Fig. 6 are two graphs (each of LTO15MF and LTO25MF) between thickness $\langle d \rangle$ and the peak location z_F of the corresponding $p_s(z)$ signal for each of the 8 different samples. Because of its bigger beam cross-section, the use of the LTO15MF resulted in a larger effective NA for the confocal microscope. To within the thickness uncertainties associated with the sample manufacture, the linear relation between distance z and thickness d for $n_s = 1.523$, as described by Eq. (1), is obeyed quite well. Also shown are theoretical z_F vs. $\langle d \rangle$ curves that were computed using Eq. (1). The effective NA of the imaging system is lower than NA = 0.25 because the SL beams did not uniformly illuminate the objective aperture.

C. Imaging of Phase Objects

We also assessed the ability of our technique to discriminate optical path differences at submillimetric lateral resolutions, by measuring the $I_{PD}(x, z = 0)$ signal produced when scanning (along the x-axis) a ridge sample that is formed by the edges of two closely-spaced cover glasses (no. 00 and no. 5). In the central section

Table 1. Thickness of cover glasses used in the experiment[15].

Cover Glass No.	d(mm)	$\langle d \rangle$(μm)
00	0.06 ~ 0.08	70
0	0.08 ~ 0.12	110
1	0.12 ~ 0.17	154
1S	0.15 ~ 0.18	178
2	0.17 ~ 0.25	228
3	0.25 ~ 0.35	308
4	0.35 ~ 0.45	406
5	0.45 ~ 0.60	536

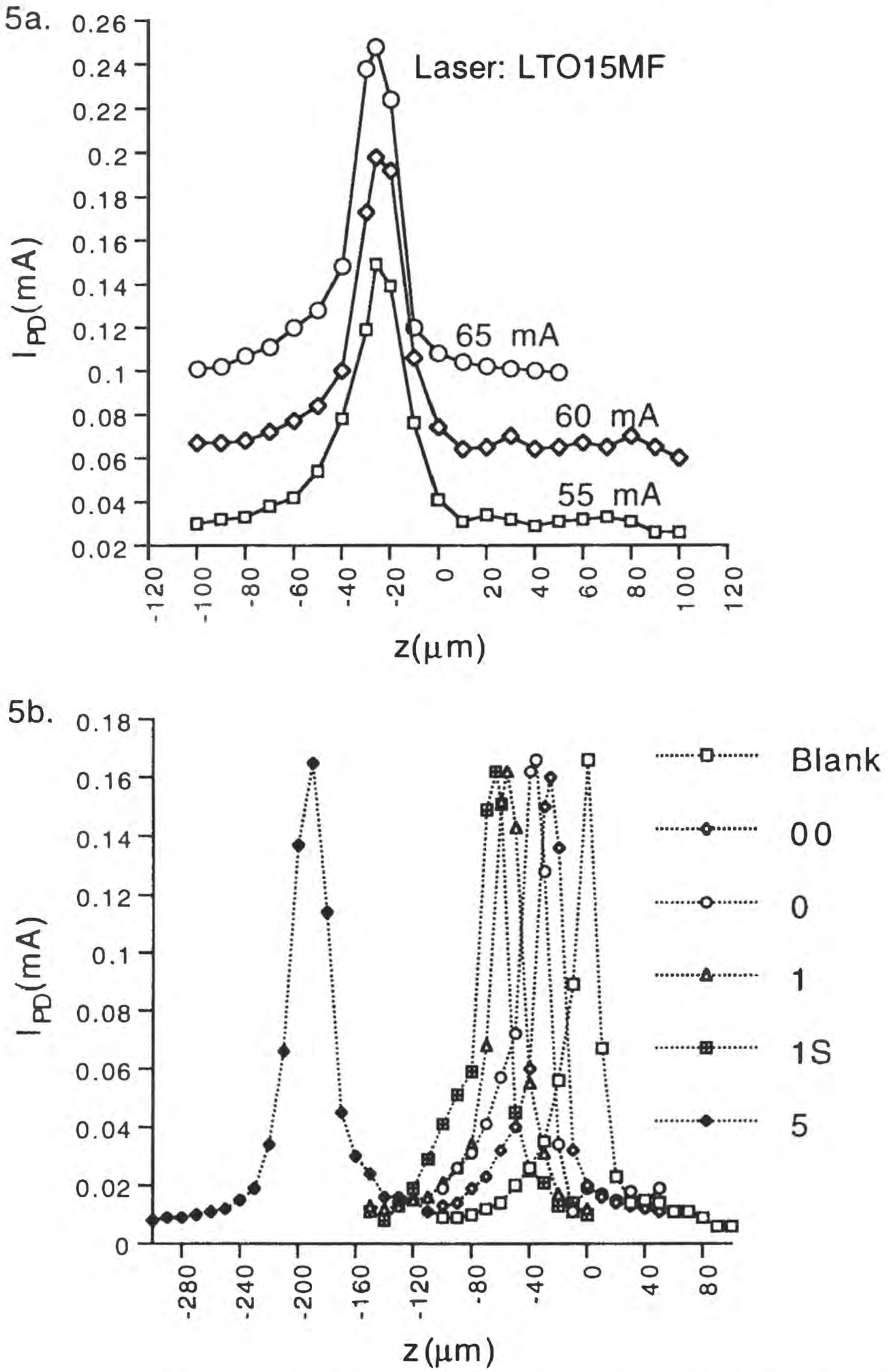

Figure 5. Axial response $I_{PD}(z)$ in the presence of: (a) sample no. 00 when I_b = 55, 60 and 65 mA; and (b) samples nos. 00, 0, 1, 1S, and 5 when I_b = 65 mA. Also shown in the axial response (blank) when no sample is present. The data shown in Fig. 6a. are not background-corrected.

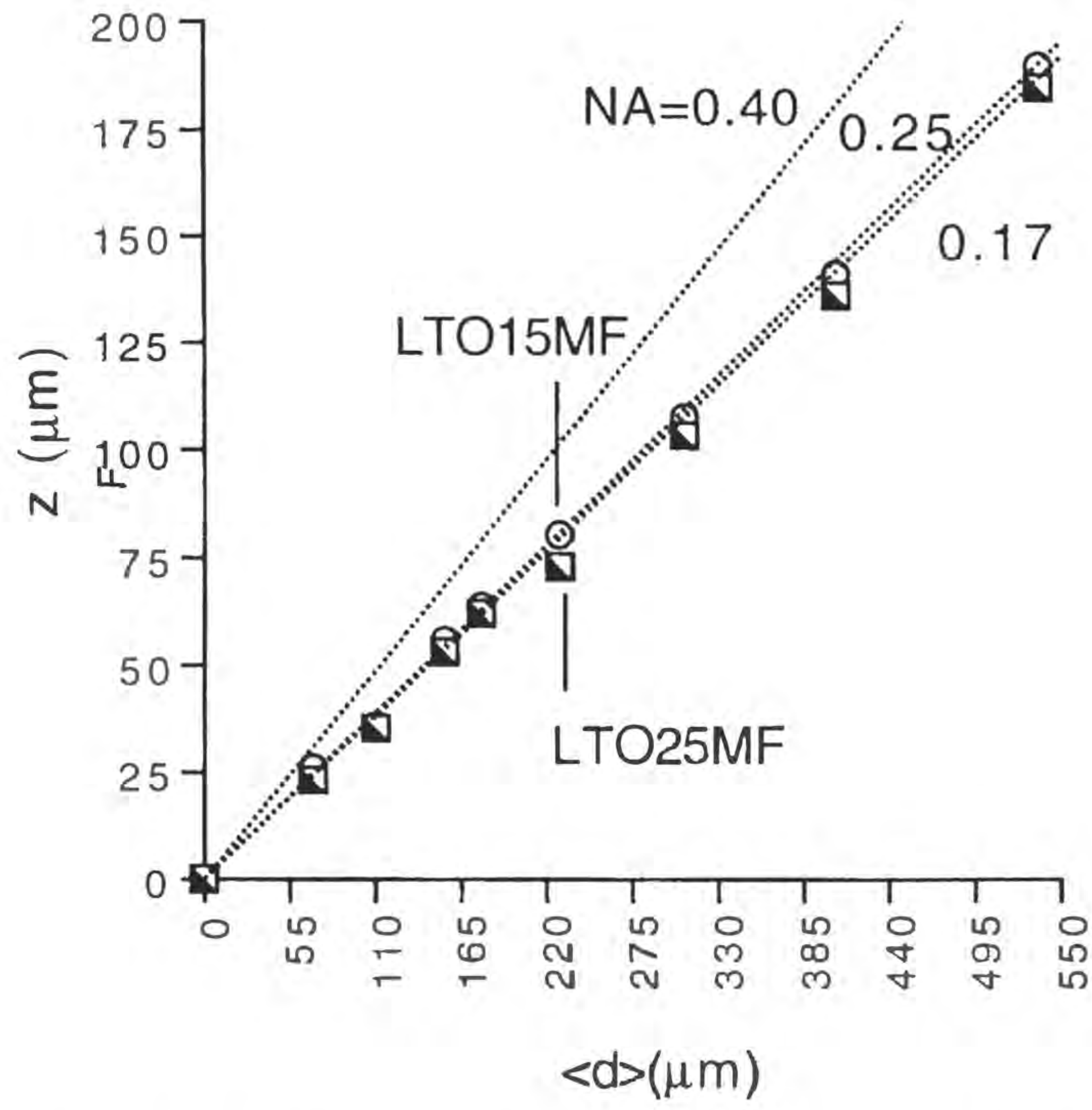

Figure 6. Graph between the measured displacement z_F and the geometrical thickness <d> of the samples listed in the Table. Also shown are the theoretical z_F vs. d curves corresponding to NA = 0.40, 0.25, and 0.17.

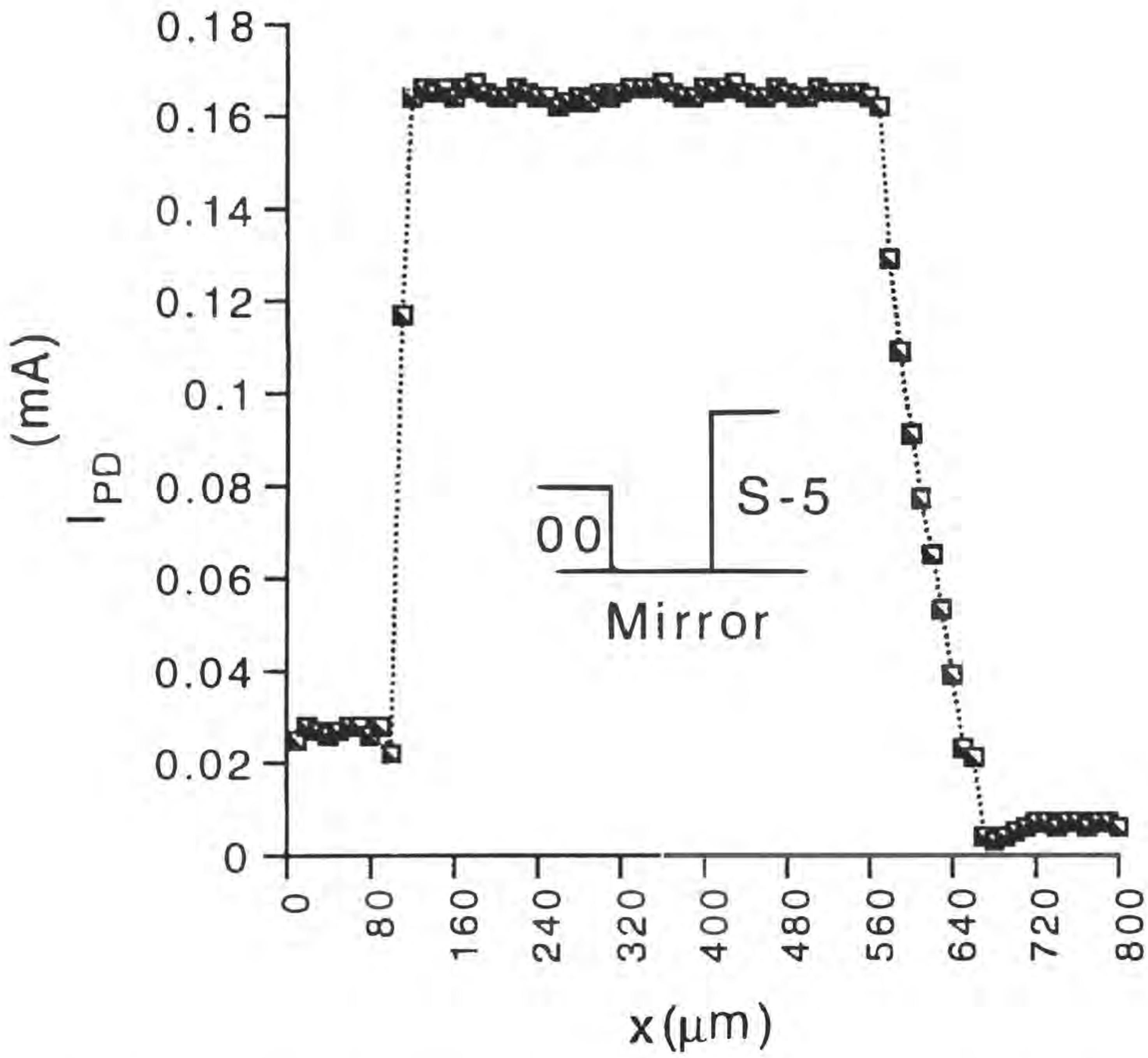

Figure 7. Background-corrected behavior of $I_{PD}(x, z = 0)$ when a phase ridge sample is scanned along the x-axis (I_b = 65 mA, LTO15MF). The ridge is bounded by cover glasses no. 00 and 5. In the central section of the ridge, the beam focus coincides with the mirror plane.

of the (phase) ridge, the beam focuses on the mirror plane and optical feedback is optimal.

In Fig. 7 is the background-corrected behavior of $I_{PD}(x, z = 0)$ as we scanned the ridge from left to right along the x-axis using LTO15MF as light source. The three sections of the ridge can be distinguished clearly from each other because of their differing optical thicknesses. In the boundaries of the central section, the probe beam is scattered by the edges of the bounding cover glasses resulting in a pair of signal dips in the vicinity of $x = 100$ µm and $x = 660$ µm. The width of the central section can be approximated from the separation distance of these dips. The edge of the thicker sample no. 5 produces a shallower dip because of the detection limit in the axial response.

We have presented a new technique of measuring minute optical path differences at microscopic transverse resolutions. When its geometrical thickness is known, the technique can be used to measure the unknown n_s of the sample, and vice-versa. The technique utilizes the optical sectioning capability of a confocal microscope, and the sensitivity of the SL output to optical feedback. Because the SL output power can be monitored efficiently by the built-in PD, the resulting laser confocal microscope is inexpensive, very easy to align, and consumes little space. The wavelength-dependence (e.g., at 640 nm, 830 nm) of $n_s(\lambda)$ can be easily determined with the use of other suitable SL packages.

REFERENCES

1. M. Pluta, "Stray-light problem in phase contrast microscopy or toward highly sensitive phase contrast devices: a review," Opt. Engineering, pp. 3199-3126 (1993).
2. H. Gundlach, "Phase contrast and differential interference contrast instrumentation and applications in cell, developmental, and marine biology," Opt. Engineering, pp. 3223-3228 (1993).
3. C. Saloma and J. Muñoz, "Refractive index measurement at high spatial resolution via source doubling," Opt. Lett. 19, pp. 1088-1090 (1994).
4. T. Wilson, ed., Confocal Microscopy (Academic Press, London, 1990), Chap. I, pp. 1-60.
5. R. Lang and K. Kobayashi, "External Optical Feedback Effects on Semiconductor Injection Laser Properties," IEEE J. Quant. Electronics, QE-16, pp. 347-355 (1980).
6. C. Saloma, S. Kawata, and S. Minami, "A Laser Diode Microscope That Generates Weakly Speckled Images," Opt. Lett., Vol. 15, pp. 203-205 (1990).
7. B. Dingel and S. Kawata, "Speckle-free image in a laser-diode microscope by using the optical feedback effect," Opt. Lett., 18, pp. 549-551 (1993).
8. R. Juskaitis, T. Wilson, and F. Reinholz, "Spatial filtering by laser detection in confocal microscopy," Opt. Lett., 18, pp. 1135-1137 (1993).
9. R. Juskaitis, N. Rea, and T. Wilson "Semiconductor laser confocal microscopy," Appl. Opt. 33, pp. 578-584 (1994).
10. D. Lenstra, M. Van Vaalen, and B. Jaskorzynska, "On the theory of a single-mode laser with weak optical feedback," Physica C, 125, pp. 255-264 (1984).

11. A.E. Seigman, Lasers (University Science, Mill Valley, CA, 1986), p. 485.
12. Databook-Creative Core Components (Sharp Corporation, Tokyo, 1992) pp. 107-109.
13. D. Lenstra, B. Verbeek, and J. den Boef, "Coherence collapse in single-mode semiconductor lasers due to optical feedback," IEEE J. Quant. Electronics, QE-21, pp. 674-679 (1985).
14. J. Mork, B. Tromborg, and J. Mark, "Chaos in Semiconductor Lasers with Optical Feedback: Theory and Experiment," IEEE J. Quant. Electronics, QE-28, pp. 93-108 (1992).
15. Matsunami Products Information (Matsunami Glass Ind., Ltd., Osaka, 1993) pp. 2-3.